SLAC-TN-03-040
LCC-0094
July 2002

Linear Collider Collaboration Tech Notes

Turbulence Induced Vibration: Theory and Application to the Next Linear Collider

Srihari Adiga

Stanford Linear Accelerator Center
Stanford University
Menlo Park, California 94025

Abstract: A semianalytical approach is used to estimate turbulence-induced vibration. The results are compared with the measured vibrations for three different cases, a 16-inch pipe at the NLCTA, a 10-inch pipe at the SLD and the coolant pipes around the copper structure model of the linear collider. The variation of vibrations with respect to velocity of flow is studied as well.

Work supported by the Department of Energy contract DE-AC03-76SF00515.

Turbulence Induced Vibration: Theory and Application to the Next Linear Collider

Srihari Adiga

Stanford University, SLAC,
2575 Sand Hill Road, Menlo Park CA 94025 , USA

LCC-Note-0094

July 2002

Abstract

A semi-analytical approach is used to estimate turbulence-induced vibration. The results are compared with the measured vibrations for three different cases, a 16-inch pipe at the NLCTA, a 10-inch pipe at the SLD and the copper accelerating structure of the Next Linear Collider.

1 Introduction

Vibrations of the components of the Next Linear Collider need to be minimized to ensure its best performance. Acoustic or mechanical resonances can be eliminated or their effects minimized by design, however, turbulence-induced vibration cannot be avoided entirely. Even though the inner surface of the coolant pipes can be extremely smooth, beyond a certain velocity called transition velocity, the flow will change from laminar to turbulent. The Reynolds (Re) number corresponding to the transition point is anywhere between 2000 and 3000. For example, for round pipe with diameter D and flow velocity V the Reynolds number is $Re = VD/\nu$ where ν is kinematic viscosity of the liquid. For example, for water at 20^oC we have $\nu \approx 10^{-6}$m^2/s (note that at 55^oC the water viscosity is already twice lower) and if the pipe diameter is $D = 1$ cm, then the flow become turbulent already above $V = 0.2$ m/s.

Fluctuating pressure in in the turbulent flow is the driving cause of vibrations. The time history of fluctuating pressure in a turbulent flow shows us that it is a random force. Thus turbulence-induced vibration is also a random process that can only be dealt with probabilistic methods. Instead of calculating detailed time history of responses, the root mean square (rms) values are estimated. It is not easily feasible to determine the turbulence forcing function by numerical techniques. The vibrational analysis is based on a combination of observed and analytical techniques. The forcing function is measured in experimental model tests and using this as input the rms responses are estimated based on probabilistic methods. Finite Element Modeling techniques can be used to estimate the responses.

In recent decades, turbulent flow induced vibrations received considerable attention, primarily because of the need to optimize design of power plants and reactors. Various models and semi-empirical techniques have been developed. In this note, following the analysis methods described and developed by Au-Yang (2001) and other authors, we will go through calculation of the turbulence induced vibrations step-by-step. The general random process formalism is described first. This is because turbulence is a random process. Since measuring the time history of turbulence is tedious, we move over to the frequency domain employing spectral analysis of random signals. The acceptance integral is defined and the assumptions made to simplify this problem are stated. We then show how these methods can be applied for analysis of experimental results relevant for the Next Linear Collider (NLC). The examples studied include measuring vibrations in the NLCTA 16 inch pipe, a 10-inch pipe at the SLD and the coolant pipes around the copper NLC accelerating structure.

2 Random process

A random process describes an experiment with outcomes being functions of a single continuous variable. (E.g. time)

Let the fluctuating pressure be a random variable p(t). The response function is a random variable y(t) : $y_i = y(t_i)$ i = 1,2,3,…n.

The mean value of y is

$$< y >= \lim_{(n\to\infty)} \frac{1}{n}\sum_{i=1}^{n} y_i$$

The Variance σ_y^2 is given by

$$\sigma_y^2 = \lim_{(n\to\infty)} \frac{1}{n}\sum_{1}^{n}(y_i- < y >)^2$$

Expanding

$$\sigma_y^2 = \lim_{(n\to\infty)} \frac{1}{n}(\sum_{1}^{n}(y_i^2)+ < y >^2 -2* < y > * \sum_{1}^{n}(y_i))$$

Since $2* < y > * \sum_1^n (y_i) = 2* < y >^2$ we get for the variance :

$$\sigma_y^2 =< y^2 > - < y >^2$$

Where $< y^2 >$ is the mean square and $< y >^2$ is the square of the mean value. The variance is important in random vibration analysis because in turbulence induced vibration, variation about the mean value is of interest only. It is reasonable to assume that mean value is zero $< y >= 0$. Hence variance is equal to the mean square value.

$$< y^2 >= \sigma_y^2 = \lim_{(n\to\infty)} \frac{1}{n}\sum_{1}^{n}(y_i- < y >)^2$$

If the mean and the mean square values are independent of the time at which we select the data points, then the random process is stationary. If each set of data points is statistically equivalent to any other set of data points irrespective of what and which time points we use, then the process is ergodic. If the mean and variance vary slowly with time then the process is quasi-stationary or quasi-ergodic. In all the calculations that follow, the process is assumed to be quasi-stationary.

When the time steps are infinitesimal, y becomes a continuous function of the time variable t. The mean and variance of the random variable y are then given by

$$< y >= \int_{-\infty}^{\infty} y f(y) dy$$

$$\sigma_y^2 = \int_{-\infty}^{\infty} (y_i - < y >)^2 f(y) dy$$

Where $f(y)$ is commonly known as the probability density function. Clearly $f(y) \geq 0$ for any y as the probability of an event occurring is always positive. We also note that $\int_{-\infty}^{\infty}$f(y) dy = 1, as the sum of all probabilities should be equal to one.

One of the solutions for $f(y)$ satisfying the above constraints is

$$f(y) = \frac{e^{-((y-<y>)^2/(2*\sigma_y^2))}}{\sqrt{2\pi\sigma_y^2}}$$

This function is called the Gaussian distribution function. It is interesting to note that the sum of statistically independent random variables follows the Gaussian distribution. This is essentially the Central Limit Theorem. Thus the rms responses that we are looking at is given by (considering the fact that the mean value of vibration is zero)

$$\sigma_y^2 = \int_{-\infty}^{\infty} y_i^2 f(y) dy$$

where f(y) is defined above.

Both the random pressure distributions as well as the distribution of the random response function of the structure follows the normal distribution. Thus the mean square pressure and the vibration amplitudes are given by

$$< p^2 >= \int_{-\infty}^{\infty} p^2 f(p) dp$$

$$< y^2 >= \int_{-\infty}^{\infty} y^2 f(y) dy$$

with $f(y)$ and $f(p)$ being the Gaussian distribution.

2.1 The use of Fourier transform and the Parseval theorem

The turbulence-induced vibration cannot be interpreted in the time domain and hence one moves over to the frequency domain. This is done through the Fourier transform. If $y(t)$ is the response function the Fourier transform is

$$Y(\omega) = \int_{-\infty}^{\infty} y(t) e^{-j\omega t}\, dt \quad \text{or} \quad Y(\omega) = \lim_{(T\to\infty)} \int_{-T}^{T} y(t) e^{-j\omega t}\, dt$$

Conversely

$$y(t) = \frac{1}{2\pi} \int_{-\infty}^{\infty} Y(\omega) e^{j\omega t}\, d\omega$$

To estimate $y^2(t)$ we use the Parseval Theorem

$$< y^2(t) >= \lim_{(T\to\infty)} \frac{1}{2T} \int_{-\infty}^{\infty} Y(\omega)Y^*(\omega)\ d\omega/(2\pi)$$

which is easy to prove taking into account that the integral over $d\omega$ will turn into a delta-function.

Suppose $S_y(\omega)$ is defined as follows

$$S_y(\omega) = \lim_{(T\to\infty)}\ \frac{1}{4\pi T}\ Y(\omega)Y^*(\omega)$$

Then the mean square of y can be written as

$$< y^2 >= \int_{-\infty}^{\infty} S_y(\omega)d\omega$$

The quantity $S_y(\omega)$ is the two sided power spectral density (PSD) of y expressed in radians/s.

It is more convenient to express the power spectral density in terms of the frequency $f = \omega/(2\pi)$ and define it only for positive values of f. Therefore we can define :

$$G_y(\omega) = 2S_y(\omega) \quad \text{for} \quad \omega \geq 0$$

Thus

$$< y^2 >= \int_{0}^{\infty} G_y(f)df$$

where $G_y(f) = 4\pi\ S_y(\omega)$ for positive values of f.

3 Acceptance integral defined and its use

A single degree of freedom spring mass system is easy to solve. However structural components like pipes are of finite spatial extent. An easy way to think about this is to consider the pipe as an infinite number of spring mass systems put together. However to solve this, we need to reduce this infinite degree of freedom systems to a finite discrete series of spring-mass systems. This can be done through what is known as modal decomposition. That is, any vibration can be decomposed into combination of normal modes and these can be summed up.

We need to calculate the response of pipes carrying turbulent flow of liquids. The responses can be thought of as mode shape functions multiplied by constants called amplitude functions.

A valid and reasonable approximation to this problem so that the problem can be simplified further is made. The surface density of the structure is assumed to be uniform, in which case, the mode shapes are orthogonal to each other.

$$\int_l \psi_m(x)\psi_n(x)dx \begin{cases} = 0 & \text{if} \quad m \neq n \\ = 1 & \text{if} \quad m = n \end{cases}$$

The usefulness of this assumption is seen later.

For a simple spring mass system excited by a force, the fourier transform yields the following result $Y(\omega) = H(\omega)*F(\omega)$, where $H(\omega)$ is the familiar transfer function defined below

$$H(\omega) = \frac{1}{[m(\omega_0^2 - \omega^2) + 2i\zeta\omega_0\omega]}$$

where ω_0 is the natural frequency of the spring mass system.

Multiplying both sides of the equation by the complex conjugates:

$$S_y(\omega) = |H(\omega)|^2 S_f(\omega)$$

In other words the power spectral density of the response is equal to the power spectral density of the forcing function multiplied by the modulus squared of the transfer function. This is a simple equation that gets complicated if the forcing function is a random function. As mentioned earlier we attempt to calculate the mean square value of the response instead of the time history of response. Moreover in our case we have a finite spatial extent excited by a spatially distributed random pressure. We use the acceptance integral method formulated by Powell (1958).

Compare the following equation to the spring mass system described above

$$m_\alpha(d^2 a_\alpha(t)/dt) + 2\omega_\alpha m_\alpha \zeta_\alpha(da_\alpha(t)/dt) + k_\alpha a_\alpha(t) = P_\alpha(t)$$

where α is the mode of vibration and $m_\alpha = \int_A \psi_\alpha(x)\, m(x)\, \psi_\alpha(x) dx$ is the generalized mass, $P_\alpha = \int_A \psi_\alpha(x)\, p(x,t) dx$ is the generalized force, $a_\alpha(t)$ is the amplitude function (of vibrations), ζ_α is the damping factor, $k_\alpha = m_\alpha \omega_\alpha^2$ and ω_α is the natural frequency of the mode α^{th}.

Fourier transforming the above equation we get

$$A_\alpha(\omega) = H_\alpha(\omega) P_\alpha(\omega)$$

where $A_\alpha(\omega)$ is the Fourier Transform of $a_\alpha(t)$, H is the modal transfer function and $P_\alpha(\omega) = \int_{-\infty}^{\infty} P_\alpha(x,t) e^{-j\omega t} dt$ is the Fourier component of the generalized pressure.

Multiplying both sides of the equation by the complex conjugates we get:

$$S_y(\omega) = (H_\alpha(\omega))^2 S_p(\omega)$$

Substituting from the above equations and from Parseval theorem we get the following expression:

$$S_y(x,\omega) = \Sigma_\alpha \Sigma_\beta H_\alpha(\omega) H_\beta^*(\omega) \frac{1}{4\pi T} \int_A dx' \int_A dx'' \psi_\alpha(x') \int_{-T}^{T} \int_{-T}^{T} p(x')p(x'') e^{-j\omega(t''-t')} dt' dt'' \psi_\beta(x'')$$

in the $\lim T \to \infty$. Here the "H" terms are the transfer functions and the ψ terms are the mode shape functions.

If the random pressure due to turbulence is completely uncorrelated between any two points then the structure will not vibrate. The only way a random pressure can excite a structure is if there is nonzero correlation in the forcing function at different points. The cross-correlation in the forcing function at different points on the structure is given by

$$R_p(x', x'', \tau) = \lim_{(T\to\infty)} \frac{1}{2T} \int_{-T}^{T} p(x', t')\, p(x'', t' + \tau) dt'$$

The fourier transform of the correlation function is

$$S_p(x', x'', \omega) = \frac{1}{2\pi} \int_{-\infty}^{\infty} R_p(x', x'', \tau)\, e^{-j\omega\tau}\, d\tau$$

When $x'' = x'$ we have the autocorrelation function. The Fourier transform of the autocorrelation is just the PSD.

With all these definitions, we rewrite the equation for $S_y(x,\omega)$ as

$$S_y(x,\omega) = A\, S_p(\omega)\, \Sigma_\alpha \psi_\alpha(x)\, H_\alpha(\omega) H^*_\alpha(\omega)\, \psi_\alpha(x) J_{\alpha\alpha}(\omega)$$
$$+ 2A\, S_p(\omega)\, \Sigma_{\alpha\neq\beta}\, \psi_\alpha(x)\, H_\alpha(\omega)\, H^*_\beta(\omega)\, \psi_\beta(x)\, J_{\alpha\beta}(\omega)$$

where α, β are counted once and A being the surface of the structure (or the length in case of one-dimensional structure).

Here $J_{\alpha\beta}(\omega)$ is the acceptance integral. When $\alpha = \beta$, then $J_{\alpha\alpha}$ is called the joint acceptance, and when $\alpha \neq \beta$ then $J_{\alpha\beta}$ is known as the cross-acceptance. The acceptance integral can be written as

$$J_{\alpha\beta}(\omega) = \frac{1}{A} \int_A \int_A \psi_\alpha(x')\, \frac{S_p(x', x'', \omega)}{S_p(x', \omega)}\, \psi_\beta(x'')\, dx'dx''$$

The acceptance integral can be understood as the measure of the probability that under the excitation of the forcing function $S_p(x', x'', \omega)$, a structure originally vibrating in the α^{th} mode will change to the β^{th} mode. The joint acceptance $J_{\alpha\alpha}$ can be defined as the probability that the structure originally vibrating in the α^{th} mode will remain in the α^{th} mode under the excitation of the force. As we see later, lesser the probability, lower the magnitude of vibrations. Essentially, it can be said that the acceptance integral has something to do with the matching of the spatial distribution of the forcing function and the mode shapes of the structure.

In the above given equation the $S_p(x', x'', \omega)$ and $S_p(x', \omega)$ are the cross-spectral density between two points x' and x'' (which are vectors, in general), and the power spectral density at x' respectively. The quantity A in general can represent the surface of a 2-D structure or the length of a one-dimensional structure. We consider a 1-D structure in our case. The integration is over the entire structure exposed to the flow excitation. So for a 1-D structure J is a double integral.

3.1 Coherence function and mean square response

The coherence function is denoted as $\Gamma(x', x'', \omega)$. It can be written as

$$\Gamma(x', x'', \omega) = \frac{S_p(x', x'', \omega)}{S_p(x', \omega)}$$

Based on appropriate boundary conditions $\Gamma \to 1$ as x' approaches x'' and $\Gamma \to \infty$ as x' moves away from x'', it is assumed that the coherence function can be written as

$$\Gamma(x', x'', f) = e^{-(2|x_1^{'} - x_1^{''}|\,/\,\lambda_1)}\, e^{-(2i\pi\, f(x_1^{'} - x_1^{''})/U_c)}$$

The above function assumes that the flow is in the x_1 direction. The first factor governs the coherence range of the forcing function. The larger the λ, the larger the coherence range of the forcing function. If λ approaches ∞, the forcing function is completely coherent with the length of the structure. Thus λ is called the correlation length of the forcing function. The second factor denotes the phase difference of the force at points x' and x''. The quantity U_c is commonly called the convective velocity. It is a measure of how fast the turbulent eddies are carried down the stream.

With the coherence function expressed by the above-mentioned formulae, the acceptance integral can be calculated by brute force numerical double integration. For certain cases this integral was tabulated. In the following, we will use the tabulated form as given by Bull (1967) for rectangular panels. The data are tabulated in form of plots of the acceptance integral versus the combination of frequency, length of the panel and convective velocity (fL/U_c) and on the boundary layer thickness normalized to the length δ^*/L.

The mean square response is obtained by integrating the response power spectral density over the entire frequency range. Thus we have

$$\begin{aligned} G_y(x,f) = &\; A\, G_p(f)\, \Sigma_\alpha\, \psi_\alpha(x)\, H_\alpha(f)\, H^*_\alpha(f)\, \psi_\alpha(x) J_{\alpha\alpha}(f) \\ &+ 2\, A\, G_p(f)\, \Sigma_{\alpha\neq\beta}\, \psi_\alpha(x)\, H_\alpha(f) H^*_\beta(f)\, \psi_\beta(x)\, J_{\alpha\beta}(f) \end{aligned}$$

where

$$H_\alpha(f) = \frac{1}{(2\pi)^2\, m_\alpha((f_\alpha^2 - f^2) + 2i\,\zeta_\alpha f_\alpha f)}$$

At this point, we could evaluate the joint and the cross-acceptances by numerical double integration at different frequency intervals and proceed to calculate the mean square response. This will account for the cross-term and the off-resonance contributions to the response. However this approach is tedious. To make estimations of the turbulence induced vibration, we shall make the following simplifying assumptions

3.1.1 Assumptions Made

– The cross-acceptances are small compared to the joint acceptances or the transfer functions H from one mode to other different modes are small compared with that from one mode to the same mode. This is true if damping is small and the normal modes are well separated.

– The forcing function is homogeneous and isotropic. That is not only power spectral density is independent of x, but also the coherence function is dependent only on the separation distance or rather the axial separation distance between any two given points.

– The acceptance integral is a slowly varying function of frequency near the natural frequencies. The mean square response is given by integrating the response PSD over ω from $-\infty$ to $+\infty$. If the modal damping is small and the normal modes are well separated most of the contribution will come from resonance peaks centered around the natural peaks.

Using the above assumptions and solving further

$$< y^2 >= \Sigma_\alpha\, A\, S_p(\omega_\alpha)\, \psi_\alpha^2(x)\, J_{\alpha\alpha}(\omega_\alpha) \int_{-\infty}^{\infty} |H_\alpha(\omega_\alpha)|^2 d\omega$$

Using contour integration and calculus of residues we can get the mean square response as :

$$< y^2 >= \Sigma_\alpha\, \pi\, A\, S_p(\omega_\alpha)\, \psi_\alpha^2(x)\, J_{\alpha\alpha}(\omega_\alpha)/(2\omega_\alpha^3\, m_\alpha^2\, \zeta_\alpha)$$

This can be written as :

$$< y^2 >= \frac{\Sigma_\alpha\, A\, G_p(f_\alpha)\, \psi_\alpha^2(x)\, J_{\alpha\alpha}(f_\alpha)}{64\,\pi^3\, f_\alpha^3\, m_\alpha^2\, \zeta_\alpha}$$

4 Empirical data used

In order to estimate quantitatively the turbulence-induced vibrations, certain empirical data need to be used. The acceptance integral depends on the boundary layer thickness, which in turn depends on the Reynolds number. The Reynolds number and boundary layer thickness relations are based on empirical data, which are described below. Depending on whether the flow has a cavitating source or not, the appropriate empirical equations for turbulence power spectral density need to be employed as well.

4.1 The displacement boundary layer thickness (δ^*) :

An estimate of the boundary layer thickness for the turbulent flow over a flat plate is

$$\delta^* = \frac{0.37\,x}{\mathrm{Re}^{1/5}}$$

where Re is the Reynolds number based on the distance x from the leading edge of the flat plate $Re = \rho V x/\mu$ (Schlichting 1979), where ρ is the density of the fluid and μ is the dynamic viscosity of the fluid ($\mu = \rho\nu$ where ν is kinematic viscosity).

In small pipes and narrow flow channels, the boundary layer fills up the entire cross-section of the flow channel:

$$\delta^* = D_H/2 = R_H$$

where D_H is the hydraulic diameter. R_H is the hydraulic radius.

In large pipes or flow channels, the boundary layer will eventually reach a final value given by (empirical):

$$\delta^* = D_H/2(n+1)$$

The value of n depends on the Reynolds number as described below in the table.

Using Navier-Stokes Momentum equations and boundary conditions at radius $r = 0$, an expression for the shear stress (varying with the radius) can be derived. We also assume that the flow is fully developed. Using this assumption, the shear stress is

$$\tau/\tau_w = r/a = (1 - y/a)$$

where a is the radius of the pipe, y is the distance measured away from the pipe wall and $\tau_w = -a/2 * dp/dx$.

It can be shown that, just like laminar flow, the pressure at a fixed cross - section is a constant. It has also been demonstrated that it is very difficult to calculate the velocity profile of a turbulent flow. Hence we make use of experimental data and empirical results.

4.2 The power-law relations

An examination of measured velocity profiles has shown that the distribution of velocity in fully developed turbulent flow can be represented by an equation of the form :

$$\frac{u}{u_{max}} = (y/a)^{1/n}$$

where u_{max} is the velocity along the axis of the pipe and hence the mean velocity U can be derived by

$$\pi a^2 U = 2\pi \int_0^a urdr = 2\pi \int_0^a U_{max}((a-r)/a)^{1/n} rdr$$

Consider the definition of friction factor $\tau_w = f * 1/2\, \rho U^2$ (where f is the friction factor, not the frequency).

The friction velocity is defined by :

$$u_\tau = (\tau_w/\rho)^{1/2}$$

From dimensional considerations

$$\frac{u}{u_\tau} = \phi(\frac{y\, u_\tau\, \rho}{\mu})$$

Comparing with the power law

$$\frac{u}{u_\tau} = K1(y\, u_\tau\, \rho/\mu)^{1/n}$$

The following table shows the variation of Re, n and $K1$

Re	n	K1
$< 10^5$	7	8.74
5*10^5	8	9.71
1.3*10^6	9	10.6
3.2*10^6	10	11.5

From the above equations it can be shown that :
friction factor **f** = $K4 * (Re)^{-2/(n+1)}$ where K4 = 2/K3
K3=(K2^n/2)$^{2/(n+1)}$; and K2 = K1*2n^2 / ((n+1)*(2n+1))
Hence **f = 0.079*(Re)**$^{-1/4}$ when Re $< 10^5$

4.3 The convective velocity

Based on experimental data obtained from turbulent flows, the following empirical equation was derived by Chen and Wambsganss (1970). This helps measure convective velocity as a function of frequency.

$$U_c/V = 0.6 + 0.4\, e^{-2.2\,(\omega\, \delta^*/V)}$$

where δ^* is the boundary layer thickness for boundary layer flow and V the velocity of flow.

Bull (1967) suggested a slightly different equation:

$$U_c/V = 0.59 + 0.3\, e^{-0.89(\omega\, \delta^*/V)}$$

which is used for our vibration calculations, to ensure continuity, because we also use Bull's empirical formulas to calculate the acceptance integrals. However both equations are more or less the same in most practical cases, when the convective velocity is about 0.6 of the flow velocity.

4.4 Turbulence random pressure power spectral density

The most important fluid mechanical parameter that characterizes the turbulent forcing function is the power spectral density. Figure.1 reproduced from Chen (1985), shows the normalized PSD as a function of non-dimensional circular frequency $(\omega\,\delta^*/V)$. This set of data is for boundary layer type flow over flat plates or in straight flow channels.

While calculating the vibrations measured in the Excel spreadsheet (described further below), a curve fit was done to generate the following empirical equation

$$Log(y) = -2.1672\,Log(x) - 4.8544$$

where y is $(\phi_{pp}(\omega)\ /\ \rho^2 \mathrm{V}^3 \delta^*)$ and x is $(\omega\delta^*/V)$. Here δ^* is the displacement boundary layer thickness as defined previously. For small pipes and narrow flow channels the displacement boundary layer thickness is the hydraulic radius itself. This curve fit has a coefficient of goodness of fit (R^2) equal to 0.87. This proves that a linear fit is a good one. The coefficient of goodness of fit explains how much the variance of the independent variable depends on the dependent variable i.e. the variance of $Log(y)$ as explained by the variance of $Log(x)$.

As pointed out by Chen (1985), the data in Figure.1 is unreliable in the low-frequency region marked effective range. Chen suggested the following empirical formulation for the low-frequency PSD:

$$(G_p(f)/\rho^2 V^3 D_H) = 0.272\ exp(-5/S^{0.25}) \quad \text{, if} \quad S > 5$$

$$(G_p(f)/\rho^2 V^3 D_H) = 22.75\ exp(-5/S^{3}) \quad \text{, if} \quad S < 5$$

where $S = 2\pi f D_H/V$.

For industry flows, there is a different set of observations. Industrial piping systems very often contain elbows and 90-degree turns and may have valves installed in them. Cavitation may occur downstream of these elbows and valves. The turbulent PSD is generally much higher for such cases as shown by Au-Yang (1995) in Figure.2 and by Au-Yang and Jordan (1980) in Figure.3. In the 1995 test, light cavitation was observed while in the 1980 test there was no noticeable cavitation. Based on these two sets of data the following two different sets of empirical formulations for industrial flows were suggested:

$$A) \begin{cases} \frac{G_p(f)}{\rho^2 V^3 R_H} = 0.155 e^{(-3F)} & 0 < F < 1.0 \\[2ex] \frac{G_p(f)}{\rho^2 V^3 R_H} = 0.027 e^{(-1.26F)} & 1 < F < 5.0 \end{cases}$$

where $F = f R_H/V$. And

$$B) \quad \frac{G_p(f)}{\rho^2 V^3 R_H} = min\{20F^{-2}(-|x|/R_H)^{-4}, 1\}$$

or the values as calculated from A, whichever is larger, where $|x|$ is the absolute value of the distance from the cavitating source such as an elbow or a valve. The case “A” describes industrial flow without cavitation and the case “B” – industrial flow with cavitation.

In the Excel software (described further below) the equations “A” are used for the industrial flow without cavitation and the curve fit is used for non-industrial flow.

4.5 Other parameters

Other parameters needed for calculations include the mode shape function and the damping factor.

Let's assume that the pipe is simply supported with the given number of supports. For example, in the case when supports are at $|x| = L/2$, the first mode shape function is

$$\psi_1 \quad = \sqrt{2/L}\,\sin(\pi x/L)$$

the maximum displacement being $\sqrt{2/L}$.

The damping factor ζ_α is assumed to be 0.01 for all the cases considered below. This could be a conservative estimate. As the damping factor is increased, the amplitude of vibrations comes down. Specifically, the amplitude of vibrations is inversely proportional to the square root of the damping factor.

4.6 Joint acceptances

As mentioned above, the longitudinal joint acceptances can be calculated by numerical double integration or the tabulated charts can be used. Bull (1967) suggested certain empirical equations for the stream wise and cross - stream wise coherence functions, and by integrating them with mode shape functions of simply supported plate the joint acceptances for several first modes were tabulated and plotted (Au - Yang 2001 and refs. therein).

A curve fit (Figure.4) to the tabulated J_{11} was done here. Up to very large values of $4fL_1/U_c$ (namely for $4fL_1/U_c > 20$) a value of 0.008 was used for J_{11}. This is certainly just an approximation, since for very large values of $(4fL_1/U_c)$, the J_{11} could be smaller. However assuming a value of 0.008 is a conservative estimate and increases the magnitude of the vibrations calculated. For smaller values of $(4fL_1/U_c)$, the following curve fit was used: $J_{11} = 1.109 * (4fL_1/U_c)^{-1.6515}$.

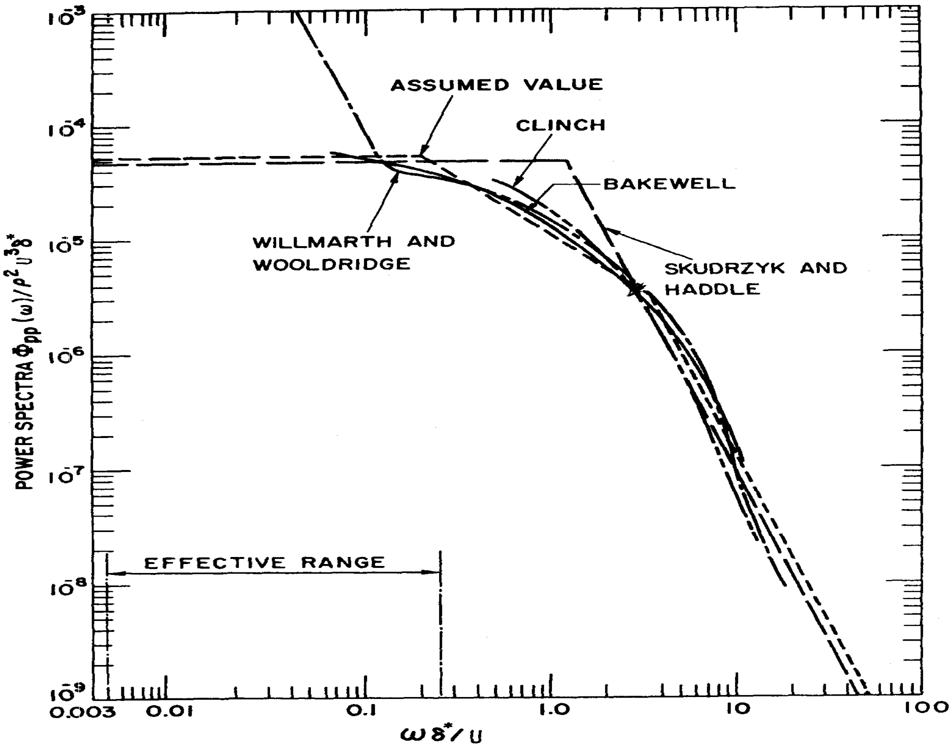

Figure 1: Turbulent Power spectral density for non-industrial flow (Chen 1985, Au-Yang 2001)

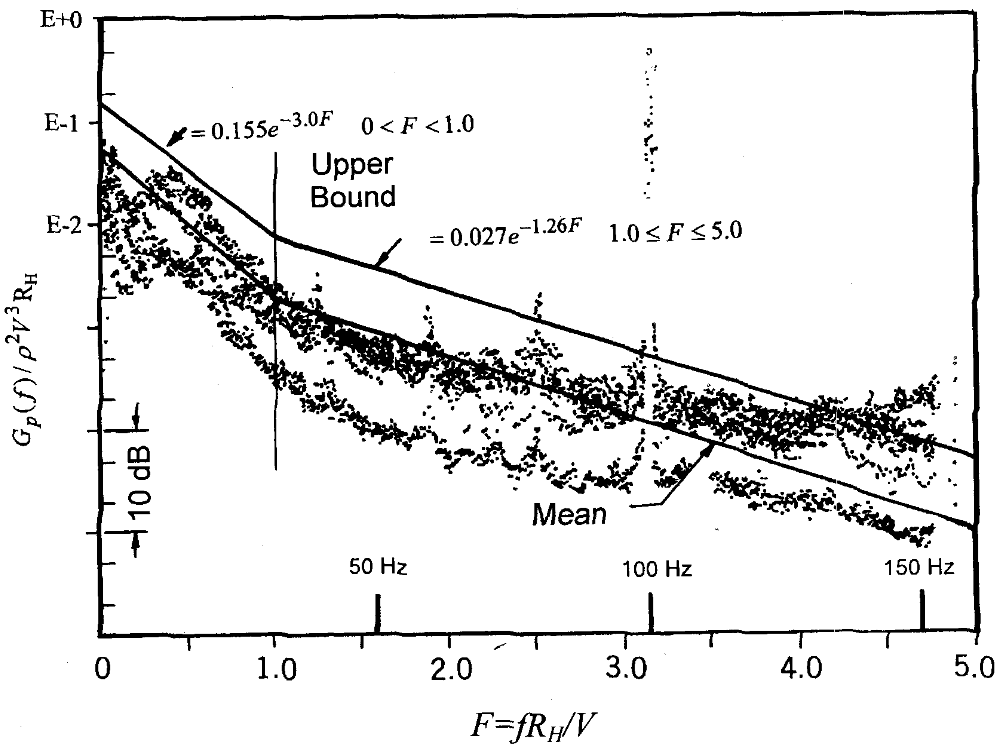

Figure 2: Comparison of empirical PSD with measured data for confined flow (Au-Yang and Jordan 1980, Au-Yang 2001)

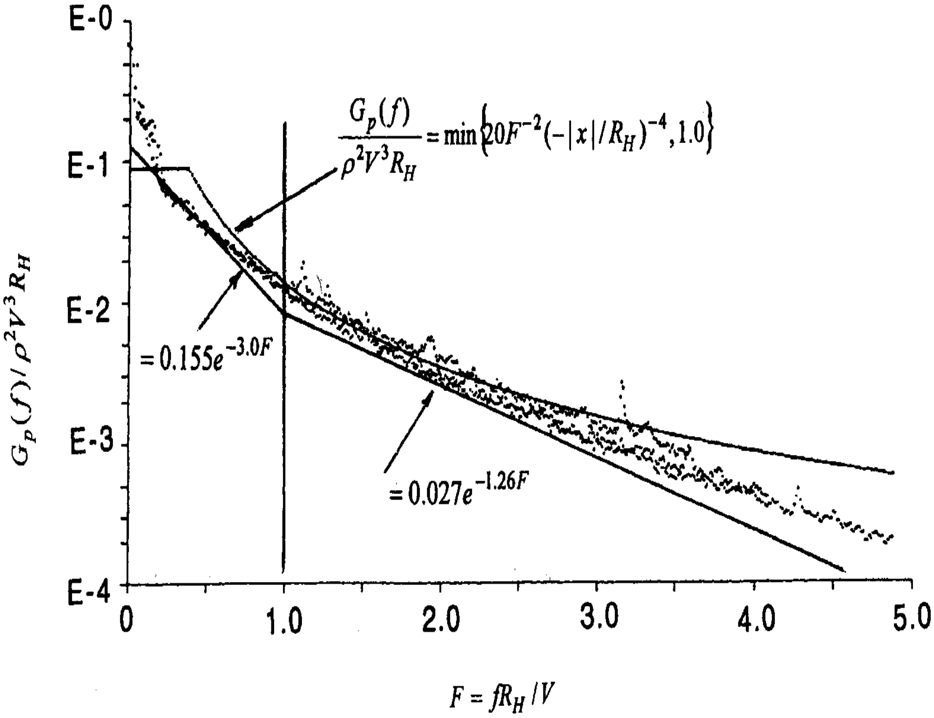

Figure 3: Comparison of empirical PSD with experimental data for turbulent flow with cavitation (Au-Yang 1985, Au-Yang 2001)

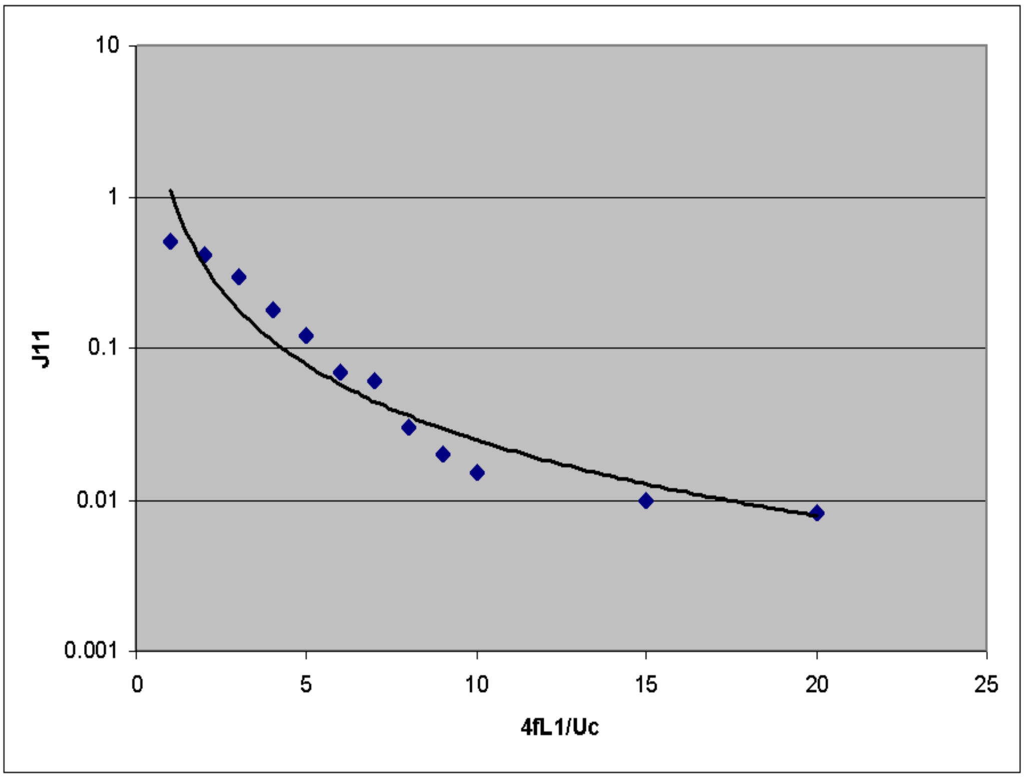

Figure 4: Semi-empirical data (symbols on the plot) for the acceptance integral $J11$ versus 4fL1/Uc (Bull 1967, Au-Yang 2001), and the fit to this data (curve).

5 Experimentally studied examples

5.1 Experiment 1: 10-inch pipe at the SLD pit

This experiment was performed in the SLD (SLAC Large Detector) pit on a 10" pipe (see Figure.6). The parameters of the experiment are the following:

Length of tube (L) = 5.5 m
Outer Diameter = 0.226 m
Density of water (ρ_w) = 1000 kg/m^3
Thickness (t) = 0.42 cm
Linear density (of tube + that of water) m$_t$: 60.5 kg/m
Stainless steel density = 8000 kg/m^3
Young's modulus (E) = 240*10^9 Pa
Hydraulic diameter (D$_H$) $= \pi$ Di^2 / πDi = 0.22 m
Velocity of flow (V) = 1 m/s
Reynolds number (Re) $\approx 2 \cdot 10^5$
Moment of inertia of the pipe (I = $\frac{\pi}{64}(D^4_{outer} - D^4_{inner})$) $\approx 1.8 \cdot 10^{-5}$ m^4
Fundamental modal frequency = (π/(2 L^2))*(E I/ m$_t$)$^{0.5}$= 13.8Hz

From the equation

$$< y^2(x = l/2) > = \frac{A\, Di^2\, G_p(f_1)\, \psi_1^2(x)\, J_{11}(f_1)}{64\, \pi^3 f_1^3\, m_\alpha^2\, \zeta_\alpha}$$

we find that $y_{rms} = 0.2\mu m$ at the center at V= 1m/s. At V= 2m/s we get 1.3μm for non-industrial flow. Note that the point where the measurements were taken was closer to the support, that could reduce the measured value. Also note that exact velocity of flow was not known and was estimated.

The measurements gave about $1\mu m$, reasonably close to predicted, considered the number of simplifications and assumptions made. The resonant frequency (step in the integrated spectrum) seem to be about 1.5 times higher than predicted.

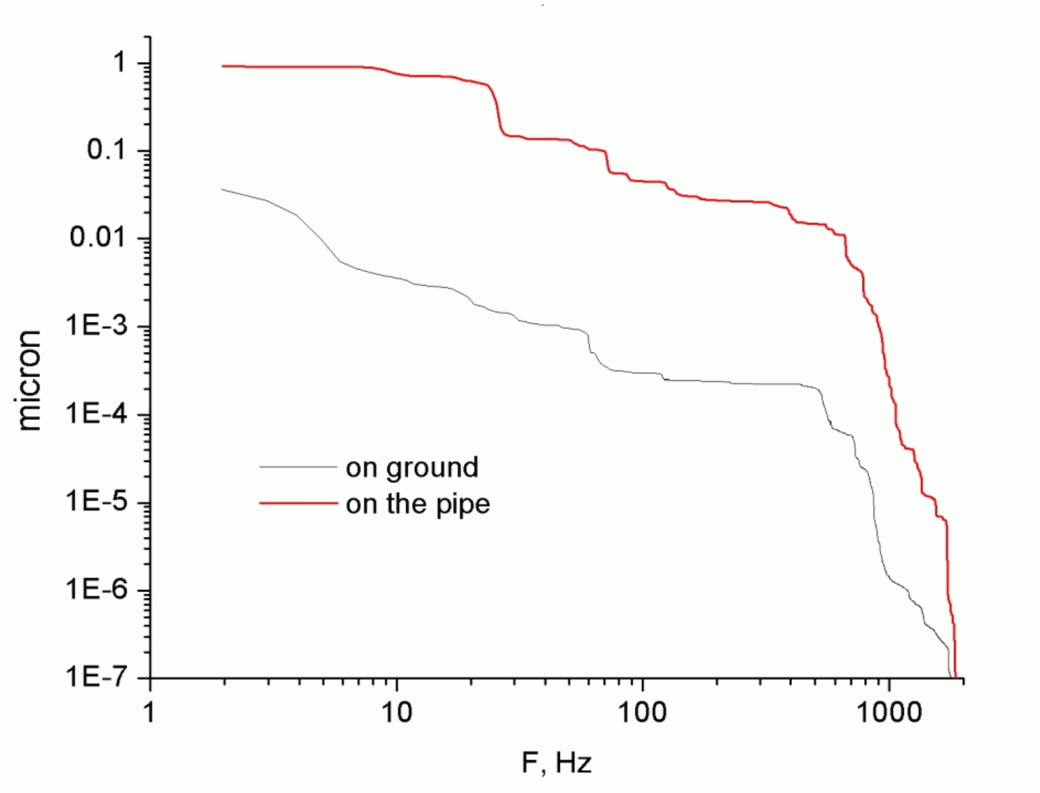

Figure 5: Example 1. Integrated spectrum of measured vibrations of a pipe in SLD pit.

Figure 6: 10 Inch Pipe at the SLD pit

5.2 Experiment 2: NLCTA 16 Inch Pipe

This experiment was performed under the NLCTA on a 16-inch pipe, see Figure.8

Length of tube: 5.28 m (distance between supports, in practice)
Velocity of Flow: 1 m/s
Diameter = 0.406 m
Density = 1000 kg/m^3
Thickness = 0.5 cm
Linear density (of tube + that of water) m_t: 173 kg/m
Stainless steel density = 8000 kg/m^3
Young's modulus = 240*10^9 Pa
Hydraulic diameter = $\pi\, Di^2/\pi Di = 0.4$
Moment of inertia of the pipe (I = $\frac{\pi}{64}(D^4_{outer} - D^4_{inner})$) $\approx 1.2 \cdot 10^{-4}$ m^4
Fundamental modal frequency = $(\pi/(2\,L^2))$*(E I/ $m_t)^{0.5}$= 24 Hz

The estimation

$$< y^2(x = l/2) >= \frac{A\, Di^2\, G_p(f_1)\, \psi_1^2(x)\, J_{11}(f_1)}{64\, \pi^3 f_1^3\, m_\alpha^2\, \zeta_\alpha}$$

gives only y_{rms}= 0.024 μm at V= 1m/s. At V= 2m/s we get 0.14 μm for non-industrial flow.

The measured vibration, as seen below in Figure.7, is close to 3 μm, much higher than the estimation. For industrial flow we get estimation of vibration magnitude is about 0.09 μm at 1 m/s and 8.5 μm at 2 m/s which is somewhat more close to the measured value.

Among the uncertainties in this case were the assumption that the tube was rigidly supported at the ends, while in practice these supports were soft.

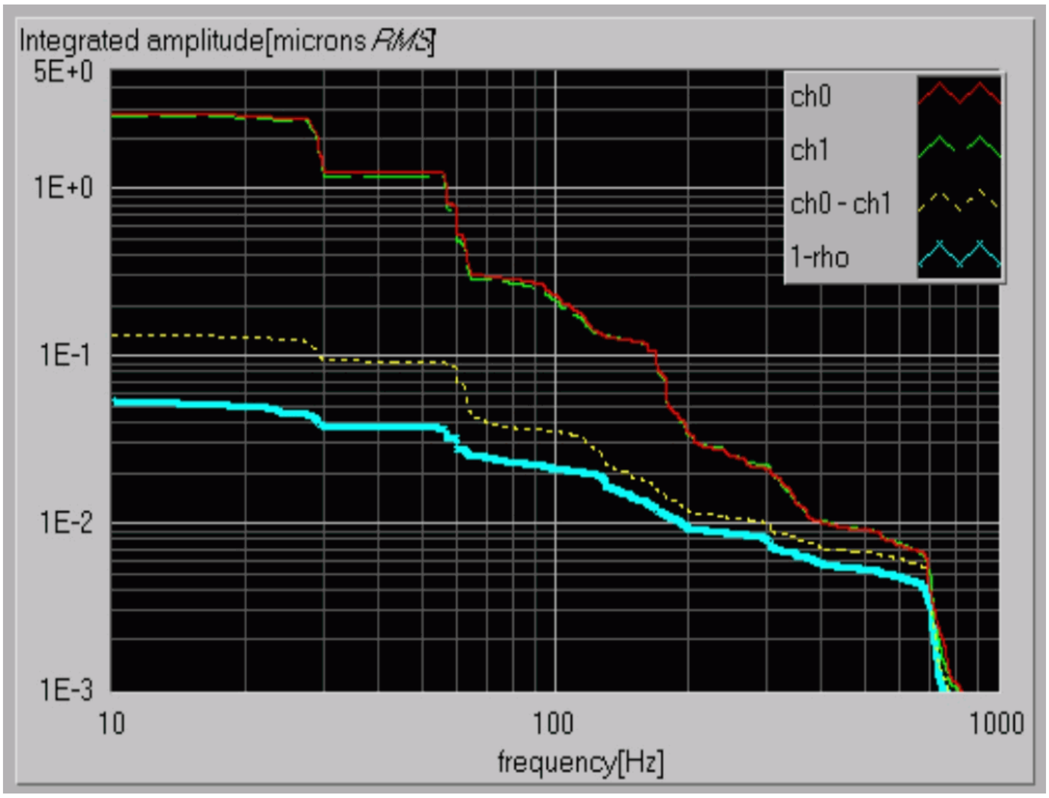

Figure 7: Example 2

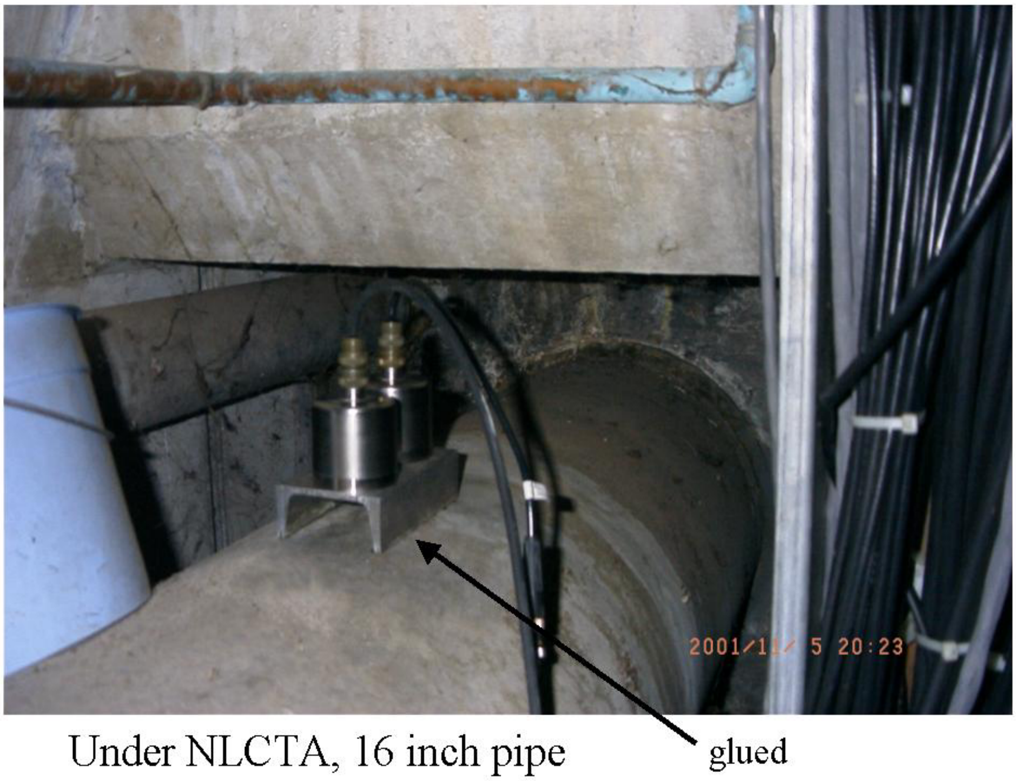

Figure 8: NLCTA 16-Inch Pipe

5.3 Experiment 3a: Vibration measurements for the coolant pipes carrying water around the copper structure.

Length of tube = 1.778m
Outer Diameter = 0.025m
Density = 1000kg/m^3
Thickness = 0.0085 m
Linear density of tube m_t: 2.493 kg/m
Copper structure density = 8230kg/m^3
Young's modulus = 120*10^9 Pa
Hydraulic diameter = π Di^2 / πDi = 0.0165m
Number of supports = 5 (=n)
Fundamental modal frequency = $(n\pi/(2L^2))*(EI/\ m_t)^{0.5}$= 217.26 Hz

We assume that the fifth mode is excited and hence we get a very high value for frequency. If this resonant frequency is not right (most likely it should be smaller than what has been calculated), we are underestimating the vibrations. However we need J_{55} and not J_{11}. In the following case, we match the frequency with what is observed and the vibrations calculated are much larger.

However the above parameters are for one cooling pipe only. We have four coolant pipes around the structure. So the total vibration from all four pipes is twice the vibration contributed from an individual pipe. The following graph, Figure.11, is the plot of the vibrations versus velocity (Obtained from the spreadsheet software, Figure.12)

The screenshot, Figure.12 above is of the Excel spreadsheet that calculates the vibrations for water flow in the coolant pipes. The vibrations are calculated as a function of velocities. The other parameters that aid in calculating vibrations are also calculated. The displacement is proportional to velocity raised to 2.5836. The vibrations should be multiplied by a factor of two to get the net displacement (as discussed previously). Moreover the coefficient of goodness (R^2) is 1 indicating a perfect fit.

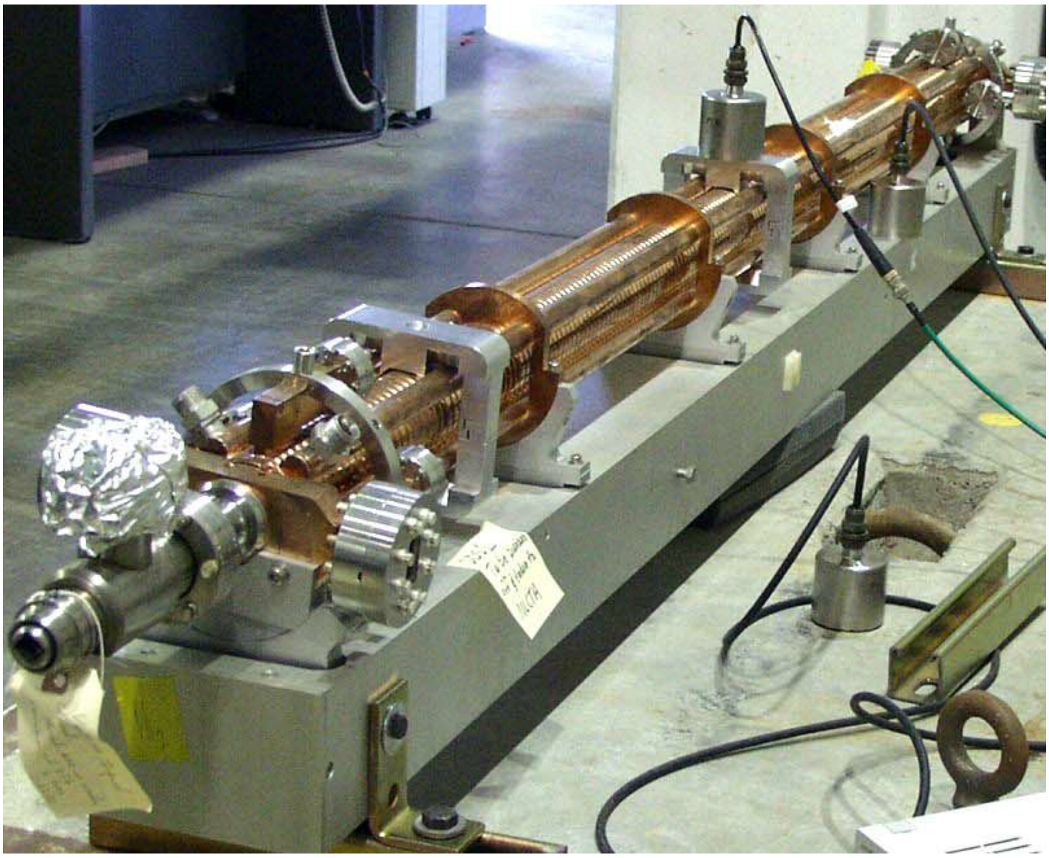

Figure 9: NLC accelerating structure

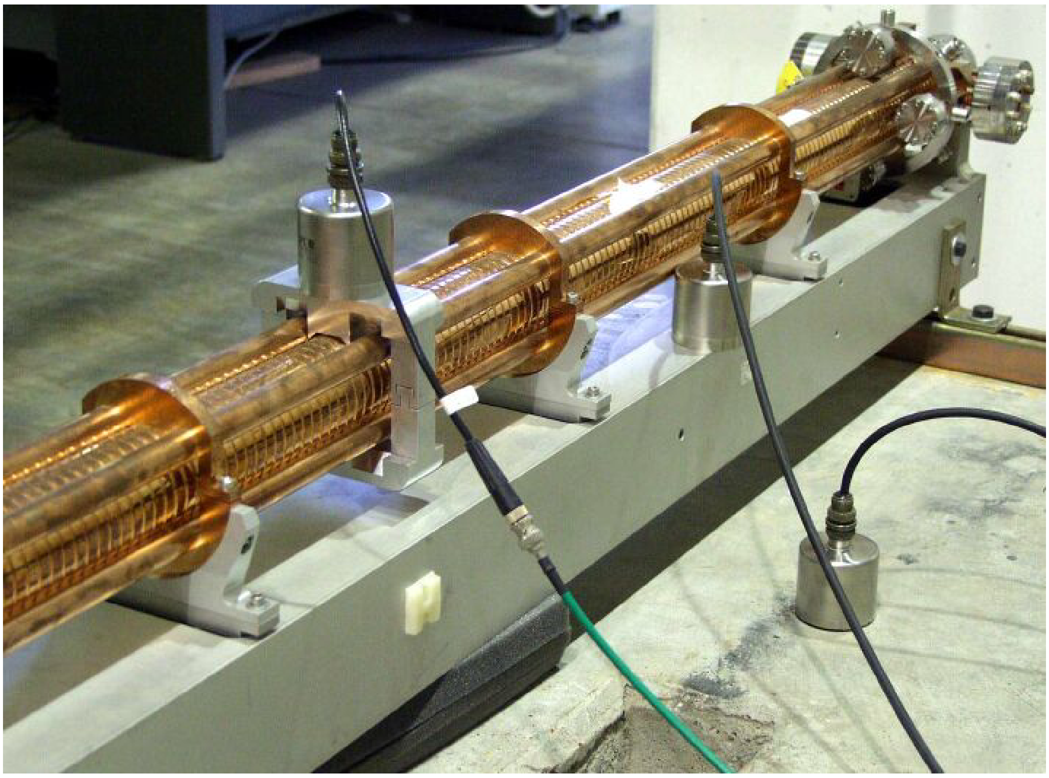

Figure 10: Closer view of the NLC accelerating structure

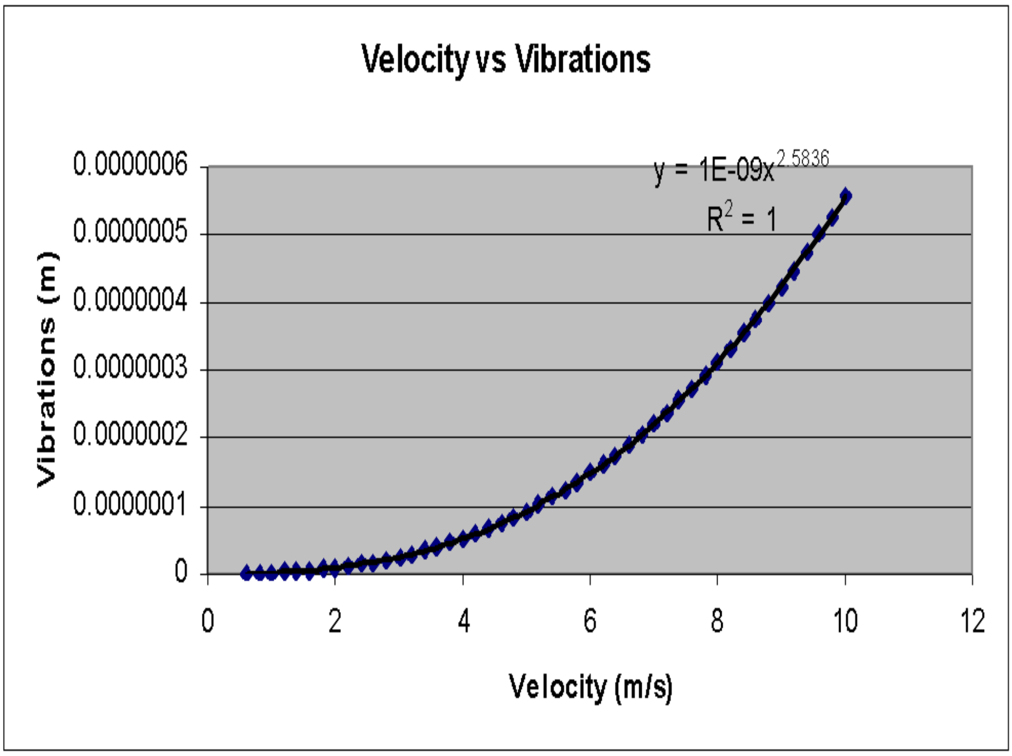

Figure 11: Plot of the velocities versus the amplitude of vibrations

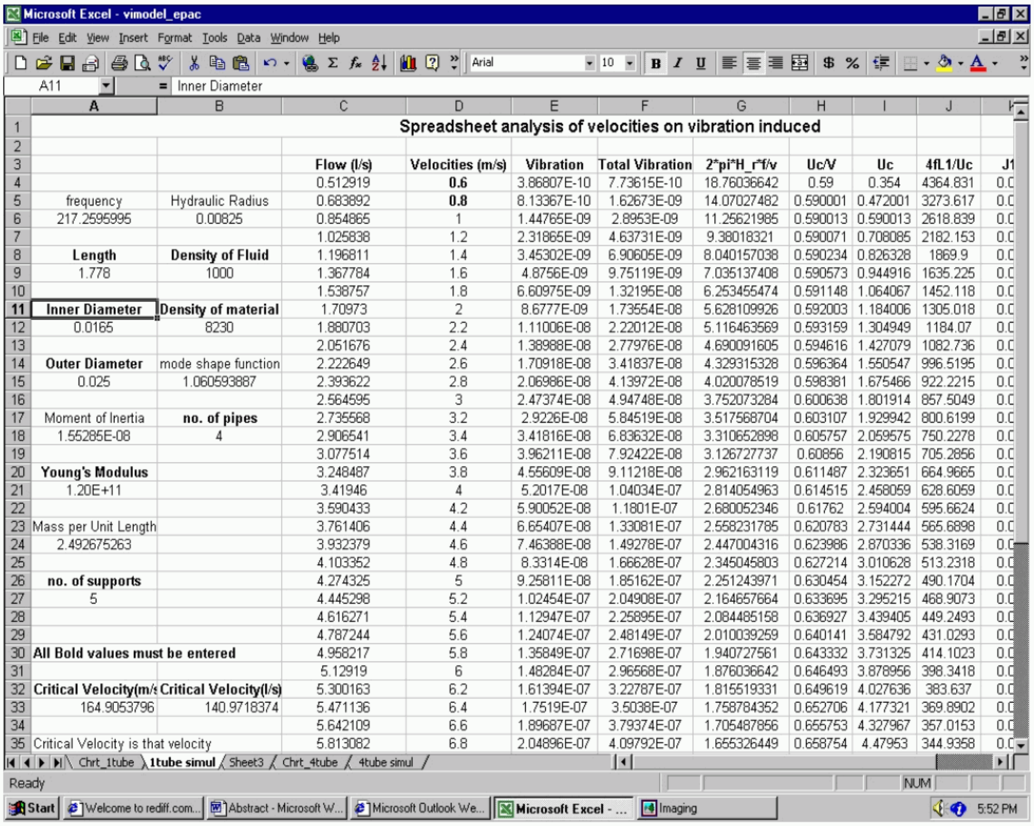

	A	B	C	D	E	F	G	H	I	J	K
1				Spreadsheet analysis of velocities on vibration induced							
2											
3			**Flow (l/s)**	**Velocities (m/s)**	**Vibration**	**Total Vibration**	**2*pi*H_r*f/v**	**Uc/V**	**Uc**	**4fL1/Uc**	**J1**
4			0.512919	**0.6**	3.86807E-10	7.73615E-10	18.76036642	0.59	0.354	4364.831	0.0
5	frequency	Hydraulic Radius	0.683892	**0.8**	8.13367E-10	1.62673E-09	14.07027482	0.590001	0.472001	3273.617	0.0
6	217.2595995	0.00825	0.854865	1	1.44765E-09	2.8953E-09	11.25621985	0.590013	0.590013	2618.839	0.0
7			1.025838	1.2	2.31865E-09	4.63731E-09	9.38018321	0.590071	0.708085	2182.153	0.0
8	**Length**	**Density of Fluid**	1.196811	1.4	3.45302E-09	6.90605E-09	8.040157038	0.590234	0.826328	1869.9	0.0
9	1.778	1000	1.367784	1.6	4.8756E-09	9.75119E-09	7.035137408	0.590573	0.944916	1635.225	0.0
10			1.538757	1.8	6.60975E-09	1.32195E-08	6.253455474	0.591148	1.064067	1452.118	0.0
11	**Inner Diameter**	**Density of material**	1.70973	2	8.6777E-09	1.73554E-08	5.628109926	0.592003	1.184006	1305.018	0.0
12	0.0165	8230	1.880703	2.2	1.11006E-08	2.22012E-08	5.116463569	0.593159	1.304949	1184.07	0.0
13			2.051676	2.4	1.38988E-08	2.77976E-08	4.690091605	0.594616	1.427079	1082.736	0.0
14	**Outer Diameter**	mode shape function	2.222649	2.6	1.70918E-08	3.41837E-08	4.329315328	0.596364	1.550547	996.5195	0.0
15	0.025	1.060593887	2.393622	2.8	2.06986E-08	4.13972E-08	4.020078519	0.598381	1.675466	922.2215	0.0
16			2.564595	3	2.47374E-08	4.94748E-08	3.752073284	0.600638	1.801914	857.5049	0.0
17	Moment of Inertia	**no. of pipes**	2.735568	3.2	2.9226E-08	5.84519E-08	3.517568704	0.603107	1.929942	800.6199	0.0
18	1.55285E-08	4	2.906541	3.4	3.41816E-08	6.83632E-08	3.310652898	0.605757	2.059575	750.2278	0.0
19			3.077514	3.6	3.96211E-08	7.92422E-08	3.126727737	0.60856	2.190815	705.2856	0.0
20	**Young's Modulus**		3.248487	3.8	4.55609E-08	9.11218E-08	2.962163119	0.611487	2.323651	664.9665	0.0
21	1.20E+11		3.41946	4	5.2017E-08	1.04034E-07	2.814054963	0.614515	2.458059	628.6059	0.0
22			3.590433	4.2	5.90052E-08	1.1801E-07	2.680052346	0.61762	2.594004	595.6624	0.0
23	Mass per Unit Length		3.761406	4.4	6.65407E-08	1.33081E-07	2.558231785	0.620783	2.731444	565.6898	0.0
24	2.492675263		3.932379	4.6	7.46388E-08	1.49278E-07	2.447004316	0.623986	2.870336	538.3169	0.0
25			4.103352	4.8	8.3314E-08	1.66628E-07	2.345045803	0.627214	3.010628	513.2318	0.0
26	**no. of supports**		4.274325	5	9.25811E-08	1.85162E-07	2.251243971	0.630454	3.152272	490.1704	0.0
27	5		4.445298	5.2	1.02454E-07	2.04908E-07	2.164657664	0.633695	3.295215	468.9073	0.0
28			4.616271	5.4	1.12947E-07	2.25895E-07	2.084485158	0.636927	3.439405	449.2493	0.0
29			4.787244	5.6	1.24074E-07	2.48149E-07	2.010039259	0.640141	3.584792	431.0293	0.0
30	**All Bold values must be entered**		4.958217	5.8	1.35849E-07	2.71698E-07	1.940727561	0.643332	3.731325	414.1023	0.0
31			5.12919	6	1.48284E-07	2.96568E-07	1.876036642	0.646493	3.878956	398.3418	0.0
32	**Critical Velocity(m/s**	**Critical Velocity(l/s)**	5.300163	6.2	1.61394E-07	3.22787E-07	1.815519331	0.649619	4.027636	383.637	0.0
33	164.9053796	140.9718374	5.471136	6.4	1.7519E-07	3.5038E-07	1.758784352	0.652706	4.177321	369.8902	0.0
34			5.642109	6.6	1.89687E-07	3.79374E-07	1.705487856	0.655753	4.327967	357.0153	0.0
35	Critical Velocity is that velocity		5.813082	6.8	2.04896E-07	4.09792E-07	1.655326449	0.658754	4.47953	344.9358	0.0

Figure 12: Excel screenshot of the vibration calculations.

5.4 Experiment 3b: Vibration measurements for the coolant pipes carrying water around the copper structure, with frequency matched with the resonance frequency

Length of tube = 1.778 m
Outer Diameter = 0.025 m
Density = 1000 kg/m^3
Thickness = 0.0085 m
Linear density of tube m_t: 2.493 kg/m
Copper structure density = 8230 kg/m^3
Young's modulus = 175*10^{10} GPa
Hydraulic diameter = π Di^2 / πDi = 0.0165m
Number of supports = 2
Fundamental modal frequency = $(\pi/2L^2)*(EI/\ m_t)^{0.5}$= 51.85 Hz

As we can see above the Young's modulus is very high, the number of supports changed to 2, so that the resonant frequency is matched with what is observed. In this case, we have the following spreadsheet Figure.14 with the calculated vibrations Figure.13. The methodology is essentially the same as 3a, the only change being matching resonant frequencies with the observed frequency.

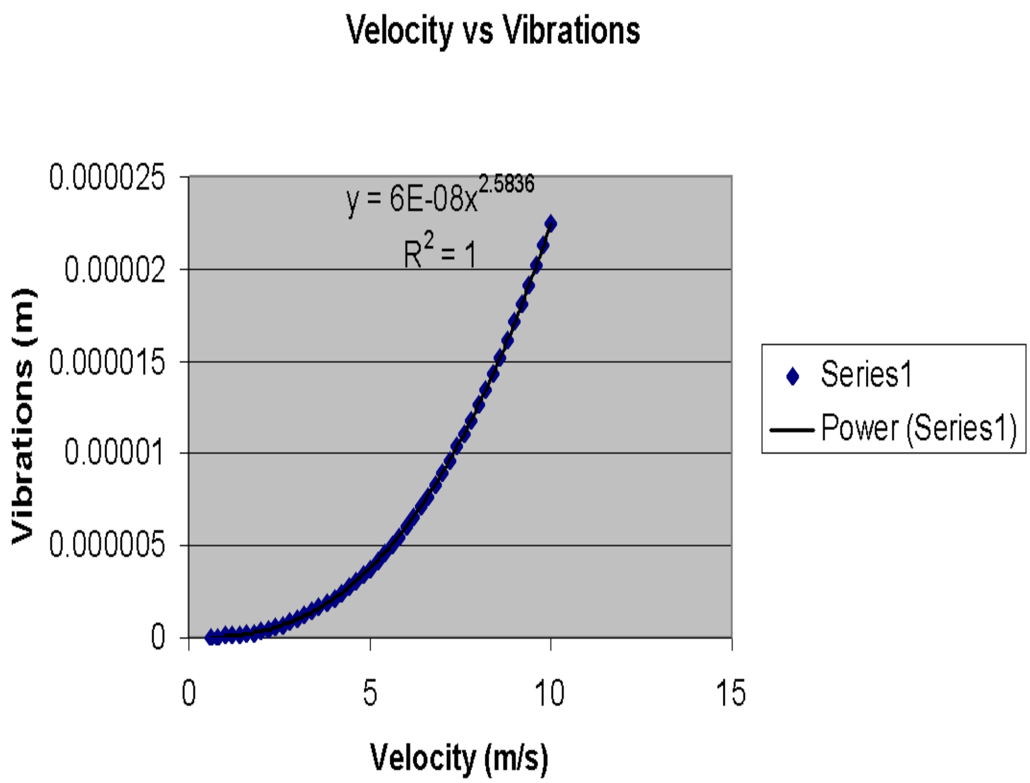

Figure 13: The plot velocity versus vibrations (higher than 3(a))

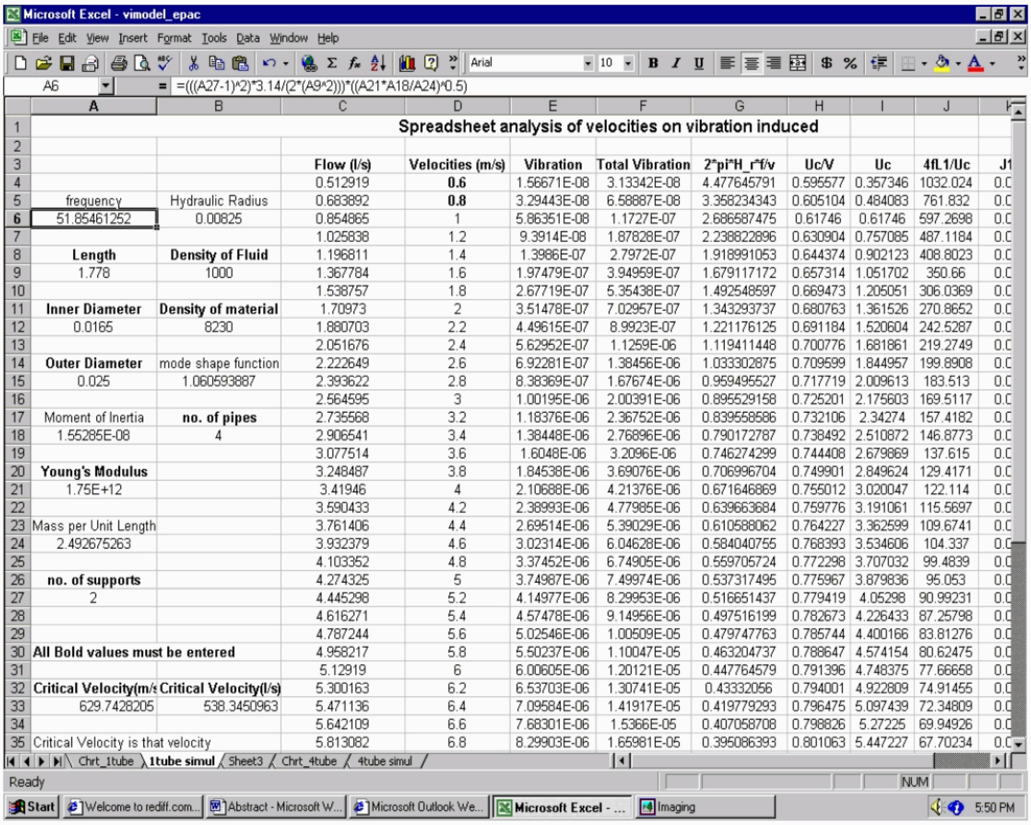

	A	B	C	D	E	F	G	H	I	J	K
1				Spreadsheet analysis of velocities on vibration induced							
2											
3			**Flow (l/s)**	**Velocities (m/s)**	**Vibration**	**Total Vibration**	**2*pi*H_r*f/v**	**Uc/V**	**Uc**	**4fL1/Uc**	**J1**
4			0.512919	**0.6**	1.56671E-08	3.13342E-08	4.477645791	0.595577	0.357346	1032.024	0.0
5	frequency	Hydraulic Radius	0.683892	**0.8**	3.29443E-08	6.58887E-08	3.358234343	0.605104	0.484083	761.832	0.0
6	51.85461252	0.00825	0.854865	1	5.86351E-08	1.1727E-07	2.686587475	0.61746	0.61746	597.2698	0.0
7			1.025838	1.2	9.3914E-08	1.87828E-07	2.238822896	0.630904	0.757085	487.1184	0.0
8	**Length**	**Density of Fluid**	1.196811	1.4	1.3986E-07	2.7972E-07	1.918991053	0.644374	0.902123	408.8023	0.0
9	1.778	1000	1.367784	1.6	1.97479E-07	3.94959E-07	1.679117172	0.657314	1.051702	350.66	0.0
10			1.538757	1.8	2.67719E-07	5.35438E-07	1.492548597	0.669473	1.205051	306.0369	0.0
11	**Inner Diameter**	**Density of material**	1.70973	2	3.51478E-07	7.02957E-07	1.343293737	0.680763	1.361526	270.8652	0.0
12	0.0165	8230	1.880703	2.2	4.49615E-07	8.9923E-07	1.221176125	0.691184	1.520604	242.5287	0.0
13			2.051676	2.4	5.62952E-07	1.1259E-06	1.119411448	0.700776	1.681861	219.2749	0.0
14	**Outer Diameter**	mode shape function	2.222649	2.6	6.92281E-07	1.38456E-06	1.033302875	0.709599	1.844957	199.8908	0.0
15	0.025	1.060593887	2.393622	2.8	8.38369E-07	1.67674E-06	0.959495527	0.717719	2.009613	183.513	0.0
16			2.564595	3	1.00195E-06	2.00391E-06	0.895529158	0.725201	2.175603	169.5117	0.0
17	Moment of Inertia	**no. of pipes**	2.735568	3.2	1.18376E-06	2.36752E-06	0.839558586	0.732106	2.34274	157.4182	0.0
18	1.55285E-08	4	2.906541	3.4	1.38448E-06	2.76896E-06	0.790172787	0.738492	2.510872	146.8773	0.0
19			3.077514	3.6	1.6048E-06	3.2096E-06	0.746274299	0.744408	2.679869	137.615	0.0
20	**Young's Modulus**		3.248487	3.8	1.84538E-06	3.69076E-06	0.706996704	0.749901	2.849624	129.4171	0.0
21	1.75E+12		3.41946	4	2.10688E-06	4.21376E-06	0.671646869	0.755012	3.020047	122.114	0.0
22			3.590433	4.2	2.38993E-06	4.77985E-06	0.639663684	0.759776	3.191061	115.5697	0.0
23	Mass per Unit Length		3.761406	4.4	2.69514E-06	5.39029E-06	0.610588062	0.764227	3.362599	109.6741	0.0
24	2.492675263		3.932379	4.6	3.02314E-06	6.04628E-06	0.584040755	0.768393	3.534606	104.337	0.0
25			4.103352	4.8	3.37452E-06	6.74905E-06	0.559705724	0.772298	3.707032	99.4839	0.0
26	**no. of supports**		4.274325	5	3.74987E-06	7.49974E-06	0.537317495	0.775967	3.879836	95.053	0.0
27	2		4.445298	5.2	4.14977E-06	8.29953E-06	0.516651437	0.779419	4.05298	90.99231	0.0
28			4.616271	5.4	4.57478E-06	9.14956E-06	0.497516199	0.782673	4.226433	87.25798	0.0
29			4.787244	5.6	5.02546E-06	1.00509E-05	0.479747763	0.785744	4.400166	83.81276	0.0
30	**All Bold values must be entered**		4.958217	5.8	5.50237E-06	1.10047E-05	0.463204737	0.788647	4.574154	80.62475	0.0
31			5.12919	6	6.00605E-06	1.20121E-05	0.447764579	0.791396	4.748375	77.66658	0.0
32	**Critical Velocity(m/s**	**Critical Velocity(l/s)**	5.300163	6.2	6.53703E-06	1.30741E-05	0.43332056	0.794001	4.922809	74.91455	0.0
33	629.7428205	538.3450963	5.471136	6.4	7.09584E-06	1.41917E-05	0.419779293	0.796475	5.097439	72.34809	0.0
34			5.642109	6.6	7.68301E-06	1.5366E-05	0.407058708	0.798826	5.27225	69.94926	0.0
35	Critical Velocity is that velocity		5.813082	6.8	8.29903E-06	1.65981E-05	0.395086393	0.801063	5.447227	67.70234	0.0

Figure 14: Excel Spreadsheet of calculated vibrations 3(b)

6 Using The Excel-Visual Basic Software

User-friendly Excel-Visual Basic software was written. The inputs include the parameters shown in the window. The outputs include the natural frequency of the pipe, critical velocity (the velocity at which the pipe buckles) and the vibrations for different velocities output on the screen. An excel macro was written to run the software from Excel, Figure.15. The software underlying the GUI (Graphic User Interface) was written in Visual Basic. The three experiments performed were discussed previously. The software takes in default values for these experiments. Otherwise the experiment specific values can also be used as inputs. The software generates a graph of velocity versus vibration as well.

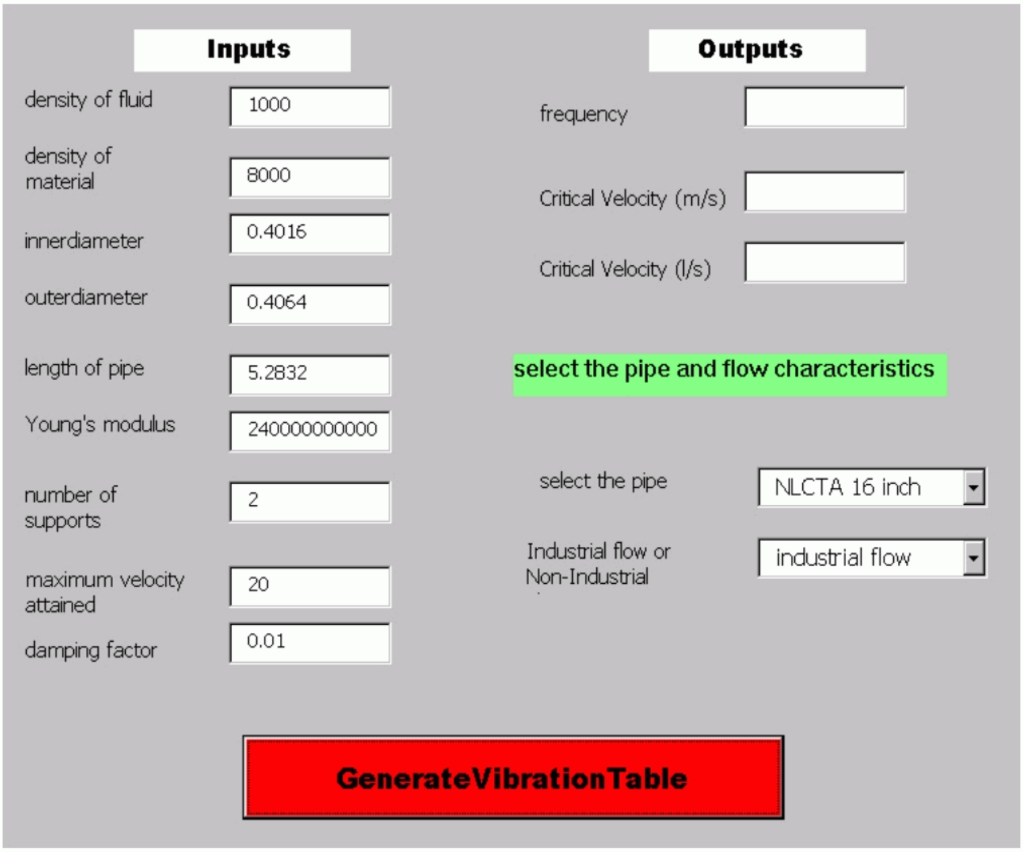

Figure 15: EXCEL-VISUAL BASIC SOFTWARE (GUI snapshot)

7 Conclusion

Vibrations induced by cooling flow have been considered in application to NLC. It was shown that semi-analytical methods allow estimating the amplitudes of turbulence induced vibrations. Predicted values agree with measurements within an order of magnitude or better. Difference may be caused by factors that are not taken into account. For example, for cavitating regime it is essential to know the distance to the cavitating source. Turbulence in the supplying pipes should also be taken into account since it can increase pressure fluctuations in the considered pipe. Therefore, though theoretical predictions can be used for rough estimations and investigations of dependencies on parameters, measurements are essential.

8 Acknowledgements

The author would like to thank Frédéric Le Pimpec, Tor Raubenheimer and Andrei Seryi for help and useful discussions.

9 References

Au-Yang, M.K., 2001, Flow-Induced Vibration of Power and Process Plant Components, A Practical Workbook, Chapters 1,2,3,8,9,10 ASME Press, New York

Au-Yang, M.K. and Jordan, K.B., 1980, “Dynamic Pressure Inside a PWR-A Study based on Laboratory and Field Test Data,” Journal Nuclear Engineering and Design, Vol. 58, pp. 113-125

Blevins R.D., 1979, Formulas for Natural Frequencies and Mode Shapes, Van Nostrand, New York

Blevins R.D., 1990, Flow Induced Vibration, Second edition, Van Nostrand Reinhold, New York

Bull M.K., 1967, “Wall-Pressure Associated with Subsonic Turbulent Boundary Layer Flow,” Journal of Fluid Mechanics, Vol 28, part 4, pp. 719-754

Chen, S.S., 1985, Flow-Induced Vibration of Circular Cylindrical Structures, Report No. ANL-85-51, Argonne National Laboratory

Schlichting Herman, 1979, “Boundary Layer Theory”, McGraw Hill, New York

Powell, A., 1958, “On the Fatigue Failure of Structures due to Vibrations Excited by Random Pressure Fields, “Journal Acoustical Society of America”, Vol 30 No 12, pp.130-1135

F. Le Pimpec, S. Adiga, F. Asiri, G. Bowden, E. Doyle, B. McKee, A. Seryi, S. Redaelli, “Vibrational Stability of NLC Linac Accelerating Structure”, EPAC 2002, Paris.